

BEAM BREAKUP INSTABILITIES IN HIGH CURRENT ELECTRON BEAM RACETRACK INDUCTION ACCELERATORS*

Brendan B. Godfrey and Thomas P. Hughes
Mission Research Corporation
1720 Randolph Road, S. E.
Albuquerque, New Mexico 87106

SUMMARY

Beam breakup and negative mass instability growth rates for a 1 kA, 40 MeV electron beam racetrack induction accelerator are computed. The device is taken to have four acceleration gaps, each with 0.2 MeV applied voltage and 15 ohm transverse impedance; the guide field is 2 kg. We find that the total amplification of the beam breakup mode is limited to five e-foldings provided that the cavity mode quality factor Q is 6. Thus, the negative mass instability, which grows several times faster, is the dominant consideration. However, we also find that the energy range over which the negative mass instability occurs can be narrowed substantially by reducing the guide field strength after the beam has been accelerated to about 12 MeV. This approach, coupled with beam thermal effects, not considered here, probably is sufficient to limit negative mass growth to acceptable levels in the racetrack accelerator.

INTRODUCTION

High current racetrack induction accelerators and modified betatrons are a subject of increasing interest as sources of high power electron beams for free electron lasers, flash radiography, and other applications. The racetrack induction accelerator geometry is illustrated schematically in Figure 1. The beam is injected from a conventional pulsed diode beam generator into the drifttube, is progressively accelerated as it repetitively passes one or more induction modules, and then is extracted from the accelerator for its intended use. Extraction may even be unnecessary for microwave applications, because a slow-wave or rippled-magnetic-field cavity can be inserted in a straight section of the drift-tube.¹

Most beam stability studies for high current recirculating devices have dealt with the negative mass and resistive wall instabilities.²⁻⁵ However, experience with linear induction accelerators suggests that beam breakup due to interaction with the induction modules and other discontinuities in the drifttube may be significant.^{6,7} The beam breakup instability arises from a resonant coupling between beam transverse oscillations and m=1 electromagnetic cavity modes localized to the acceleration gaps, resulting in large lateral displacements of the beam.^{8,9} In this paper we present a linear dispersion relation describing both beam breakup and negative mass instabilities, including their possible interaction, and evaluate it for parameters of the proposed racetrack induction accelerator designed by the Naval Research Laboratory.¹

The NRL device is based on the four module linear induction accelerator developed by the National Bureau of Standards.¹⁰ It is expected to accelerate a 1 kA electron beam from 1 to 40 MeV in fifty cycles. The beam and drifttube radii are 1 and 7 cm, respectively. The principle m=1 resonance of the gaps has a frequency of 880 MHz, an impedance of 15

ohms, and a quality factor (Q) of 60. Experience with the ETA linear induction accelerator at Lawrence Livermore National Laboratory indicates that Q can be greatly reduced, however, and we shall take Q=6 in our numerical work.¹¹ The NRL design includes a 2 kg axial magnetic field to maintain the beam equilibrium and improve beam stability at low energies. Reducing or eliminating this guide field at higher energies is nonetheless an interesting possibility. The stability analyses below consider both options.

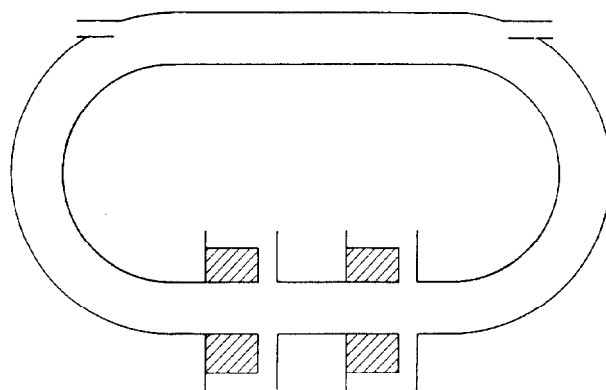


Figure 1. Simplified representation of recirculating induction accelerator with racetrack drift tube, acceleration gaps, and injection and extraction ports.

DISPERSION RELATION

For simplicity we represent the racetrack accelerator as a torus with a single gap. These two approximations are conservative in that omitting the straight sections of the racetrack and lumping the several gaps into one overestimate negative mass and beam breakup growth, respectively. The desired dispersion relation is

$$(\Omega^2 - \omega_r^2 + F_r/\gamma L + \omega_\theta^2 \ell^2 \chi) (\Omega^2 - \omega_z^2 + F_z/\gamma L) - (R_\theta/\gamma)^2 \Omega^2 = 0 \quad (1)$$

with

$$\chi = \tilde{\nu} \frac{\omega}{v_\theta} (\omega v_\theta - \frac{\ell}{R}) / [\Omega^2 + \tilde{\nu} (\omega^2 - \frac{\ell^2}{R^2})] \quad (2)$$

$$\tilde{\nu} = (1 + 2\ell n a/r_b) v/\gamma^3 \quad (3)$$

Here, $\Omega = \omega - \ell\omega_\theta$ is the Doppler-shifted wave frequency, ℓ is the toroidal mode number, and $\omega_\theta = v_\theta/R$ is the toroidal rotation frequency of the beam. (The poloidal rotation frequency is assumed negligible.) The radial and vertical betatron frequencies are

*Work supported by the Office of Naval Research.

$$\begin{aligned} \omega_r^2 &= (1 - n - n_s r_b^2/a^2) \omega_\theta^2 \\ \omega_z^2 &= (n - n_s r_b^2/a^2) \omega_\theta^2 \\ n_s &\equiv n_b / (2\omega_\theta^2 \gamma^3) \end{aligned} \tag{4}$$

with n the betatron index, n_b the beam density, $\nu = n_b r_b^2/4$ Budker's parameter, and γ the beam energy. The drifttube major radius is R , the drifttube minor radius is a , and the beam minor radius is r_b . $L=2\pi R$. The toroidal guide field strength is B_θ ; the betatron field strength enters as $B_z = -\omega_\theta R$.

In a high current betatron ω_r^2 and ω_z^2 can be of either sign. The beam is unstable, however, whenever

$$\omega_B^2 = \omega_z^2 \omega_r^2 / (B_\theta/\gamma)^2 \tag{5}$$

is negative. To avoid this situation, as well as for simplicity, we take $n=1/2$. The energy at which $\omega_B^2 = 0$ typically is labeled the transition energy,

$$\gamma_{tr} \approx (4 \nu R^2/a^2)^{1/3} \tag{6}$$

The gap response function F is defined as⁹

$$\frac{F}{\gamma} = - \frac{Z_\perp}{Q} \frac{\omega_0^3}{\omega^2 + i\omega_0 \omega / Q - \omega_0^2} \frac{\nu}{\gamma} \tag{7}$$

where ω_0 is the resonant frequency, Z_\perp/Q is the transverse impedance, and Q is the quality factor. Setting $F=0$ in (1) recovers the high current beam negative mass dispersion relation.⁴ The negative mass instability occurs for all ℓ over a broad range of energies when $\gamma > \gamma_{tr}$. For low ℓ only, one or two instability bands (often overlapping) also may exist when $\gamma < \gamma_{tr}$. Three of the six beam modes ($m=0$ spacecharge, $m=1$ spacecharge, and $m=1$ cyclotron; m is the poloidal mode number) have negative energy and so can couple unstably to the gap fields. Note that coupling in the $m=0$ spacecharge mode occurs only due to toroidal curvature. Choosing $R=70$ cm, we find maximum coupling at $\ell \approx 13$.

LARGE B ANALYSIS

For the parameters considered here and toroidal mode numbers in the vicinity of 13, the negative mass instability exists only beyond the transition energy $\gamma_{tr} \approx 2.9$. Just above the transition energy the instability is due solely to the interaction between the positive and negative energy $m=1$ spacecharge modes, while at still higher energies the $m=0$ spacecharge modes also are involved. This change is readily visible in the negative mass instability growth rate, the dashed curve in Figure 2. Which portion grows faster depends on circumstances.

Although the peak growth rate at lower energy is not readily determined analytically, the higher energy peak is easily shown to be

$$\Gamma \approx \frac{\sqrt{3}}{2} [2 \ell \omega_\theta \omega_B^2 \nu \gamma^2]^{1/3} \tag{8}$$

Instability ceases for

$$\gamma > [6\sqrt{3} \ell R B_\theta \nu (1 + 2 \ell n a/r_b)]^{1/2} \tag{9}$$

here about 62.

In the absence of curvature, the beam breakup growth rate also is easily estimated. For Q not too large,⁹

$$\Gamma \approx \omega_0 Q \frac{\nu Z_\perp/Q}{B_\theta L} \tag{10}$$

Both $m=1$ negative energy modes grow at this rate when their frequencies roughly match ω_0 .

The solid curves in Figure 2 show growth rates of the negative mass and beam breakup instabilities combined. The negative mass results are seen to be only weakly affected by the gap resonance. The $m=1$ cyclotron and hybrid $m=0/1$ spacecharge modes have become unstable, however, with a growth rate agreeing with (10) to within a factor of 1.5. These findings are insensitive to small changes in the resonant frequency.

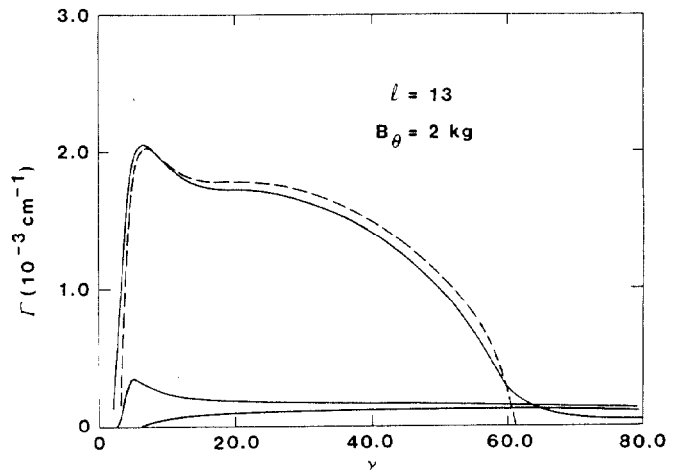


Figure 2. Combined negative mass and beam breakup instability growth rates (solid curves) for $\ell=13$ and $B_\theta=2$ kg. Growth of the negative mass instability alone (dashed curve) is included for comparison.

SMALL B ANALYSIS

Although modified betatron and racetrack induction accelerator studies usually assume a large toroidal guide field, large B_θ is in fact needed to provide a beam equilibrium only for γ small. Reducing or perhaps eliminating B_θ after the beam has been accelerated sufficiently has certain advantages for stability, as we see below.

For $B_\theta=0$, the negative mass growth rate is approximately

$$\Gamma \approx \frac{\sqrt{3}}{2} [\ell \omega_\theta^3 \nu \gamma^2]^{1/3} \tag{11}$$

This expression exceeds (8) whenever $B_\theta/\gamma > \omega_\theta$. However, the corresponding high energy cutoff,

$$\gamma > 3\sqrt{3} \ell \nu (1 + 2 \ell n a/r_b) \tag{12}$$

here 27.5, typically is much lower than (9). See the dashed curve in Figure 3.

The beam breakup instability maximum growth rate is again readily estimated, this time giving

$$\Gamma \approx \omega_0 Q \frac{v Z_1/Q}{2\omega_z L \gamma} \quad (13)$$

Equation (13) exceeds (10) for $B_\theta/\gamma > 2\omega_z$. The solid curves in Figure 3 show the effects of $F \neq 0$. As in Figure 2, the negative mass instability is only slightly modified by the gap; the beam breakup instability is described reasonably well by (13).

A comparison of the two figures suggests that some reduction in total instability growth during acceleration can be achieved by rapidly decreasing the guide field as the beam energy exceeds about 12 MeV.

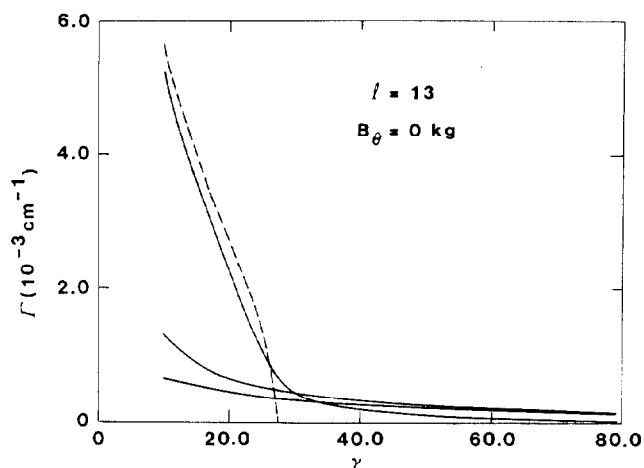


Figure 3. Combined negative mass and beam breakup instability growth rates (solid curves) for $l=13$ and $B_\theta=0$ kg. Growth of the negative mass instability alone (dashed curve) is included for comparison.

REFERENCES

1. C. W. Roberson, IEEE Nuc. Sci. NS-28, 3433 (1981).
2. P. Sprangle and J. L. Vomvoridis, NRL-4688 (Naval Research Laboratory, Washington, 1981).
3. B. B. Godfrey and T. P. Hughes, AMRC-R-332 (Mission Research Corporation, Albuquerque, 1981).
4. T. P. Hughes and B. B. Godfrey, AMRC-R-354 (Mission Research Corporation, Albuquerque, 1982).
5. B. B. Godfrey and T. P. Hughes, AMRC-N-207 (Mission Research Corporation, Albuquerque, 1982).
6. T. J. Fessenden, W. A. Atchison, D. L. Birx, R. J. Briggs, J. C. Clark, R. E. Hester, V. K. Neil, A. C. Paul, D. Rogers, and K. W. Struve, Proc. 4th Conf. Electron and Ion Beam Research Technology (Palaiseau, 1981), p. 813.
7. R. B. Miller, J. W. Poukey, B. G. Epstein, S. L. Shope, T. C. Genoni, M. Franz, B. B. Godfrey, R. J. Adler, and A. Mondelli, IEEE Nuc. Sci. NS-28, 3343 (1981).
8. V. K. Neil, L. S. Hall, and R. K. Cooper, Part. Accel. 9, 213 (1979).
9. B. B. Godfrey and T. P. Hughes, AMRC-R-410 (Mission Research Corporation, Albuquerque, 1982).
10. J. E. Leiss, N. J. Norris, and M. A. Wilson, Part. Accel. 10, 223 (1980).
11. D. L. Brix, UCID-18630 (Lawrence Livermore National Laboratory, Livermore, 1980).